Electronic Supplementary Information for:

Reaction Landscape of a Pentadentate N5-Ligated Mn^{II} Complex with $O_2^{\bullet-}$ and H_2O_2 Includes Conversion of a Peroxomanganese(III) Adduct to a Bis(*μ*-O)dimanganese(III,IV) Species

Domenick F. Leto,[a] Swarup Chattopadhyay, [a,b,c] Victor W. Day,[a] and Timothy A. Jackson[a,b]*

[a] *Department of Chemistry, University of Kansas 1251 Wescoe Hall Drive, Lawrence, KS 66045, USA. Fax: +1 785-864-5693; Tel: +1 785-864-3968; E-mail: taj@ku.edu*

[b] *Center for Environmentally Beneficial Catalysis, University of Kansas, Lawrence, KS 66045, USA*

[c] *Current address: Department of Chemistry, University of Kalyani, Kalyani, West Bengal India*

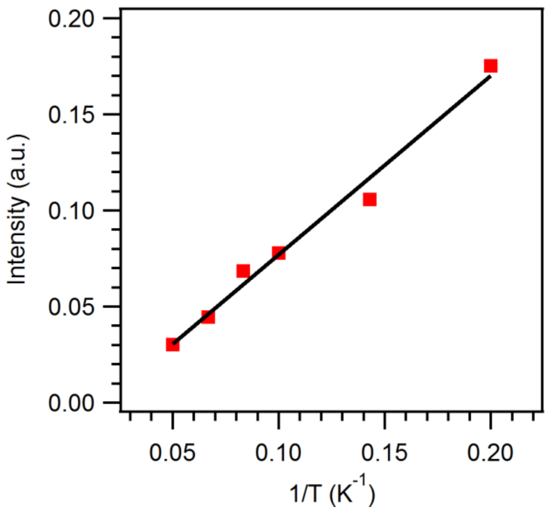

Figure S1. Temperature dependence of the parallel-mode EPR intensity (75 mT) of a 5 mM butyronitrile solution of **2** with low-field baseline correction (T = 5 – 20 K).

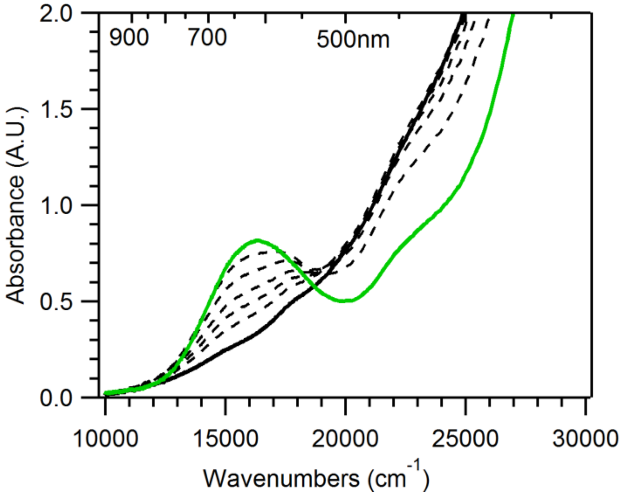

Figure S2. Electronic absorption spectra of **2** (green), formed from the addition of 2 equivalents of KO_2 to 5 mM **1** in MeCN at -20 ^{o}C, and its decay over 3 hours (black).

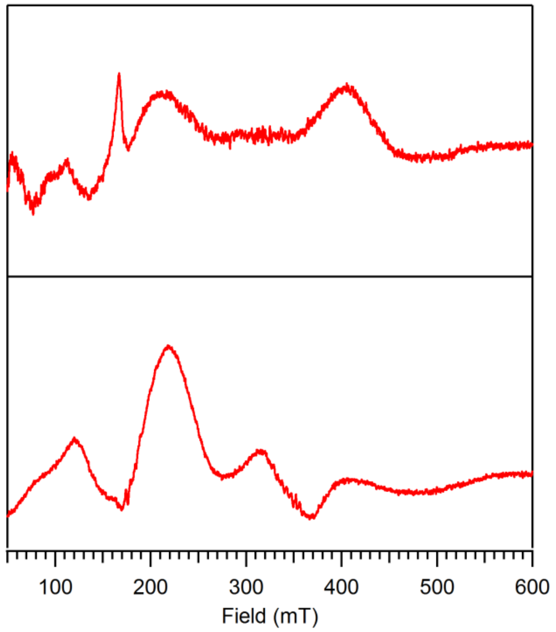

Figure S3. *Top*: Parallel-mode X-band EPR spectrum of the decay products of a 5 mM solution of **2** in butyronitrile. **2** was formed by reaction with 2 equivalents KO_2. Recording conditions: $T = 5$ K, 9.3944 GHz microwave frequency, 2.0 mW microwave power, 0.4 mT modulation amplitude, 100 kHz modulation frequency, 81.92 ms time constant, and 15 000 point resolution. *Bottom*: Perpendicular-mode X-band EPR spectrum of the same solution. Recording conditions: $T = 5$ K, 9.6369 GHz microwave frequency, 0.0317 mW microwave power, 0.4 mT modulation amplitude, 100 kHz modulation frequency, 81.92 ms time constant, and 15 000 point resolution.

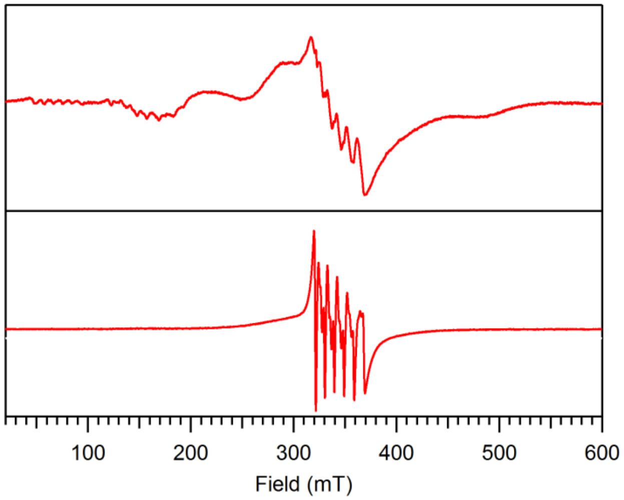

Figure S4. *Top*: Perpendicular-mode X-band EPR spectrum of a 5 mM butyronitrile solution of **1**. Recording conditions: $T = 5$ K, 9.6371 GHz microwave frequency, 0.002 mW microwave power, 0.4 mT modulation amplitude, 100 kHz modulation frequency, 81.92 ms time constant, and 15 000 point resolution. *Bottom*: Perpendicular-mode X-band EPR spectrum of 2 mM $[Mn(OTf)_2]$ in butyronitrile. Recording conditions: $T = 5$ K, 9.6369 GHz microwave frequency, 0.00796 mW microwave power, 0.4 mT modulation amplitude, 100 kHz modulation frequency, 81.92 ms time constant, and 7500 point resolution.

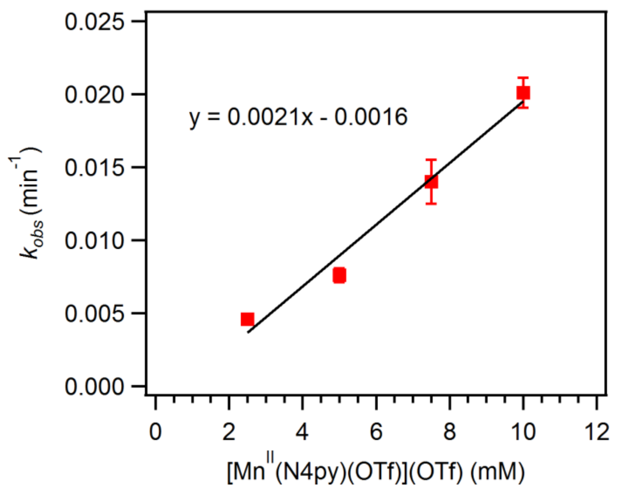

Figure S5. Observed rate constant (k_{obs}) versus the initial concentration of **1**, at -40 °C in MeCN. The k_{obs} values were determined by optically monitoring the rate of formation of **3** at 17 700 cm^{-1}. Error bars represent ±1 standard deviation.

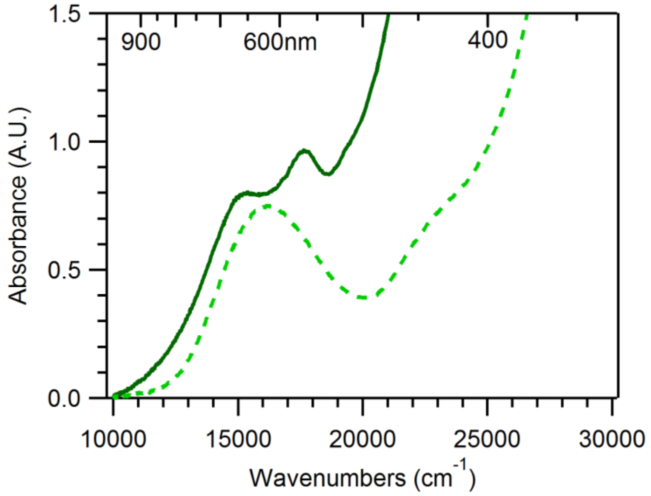

Figure S6. Electronic absorption spectra of a 5 mM acetonitrile solution of $[Mn^{III}(O_2)(N4py)]^+$ (**2**) before (green dashed line) and after the addition of one equiv. $[Mn^{II}(N4py)(OTf)](OTf)$ (solid dark green line) at -40 °C.

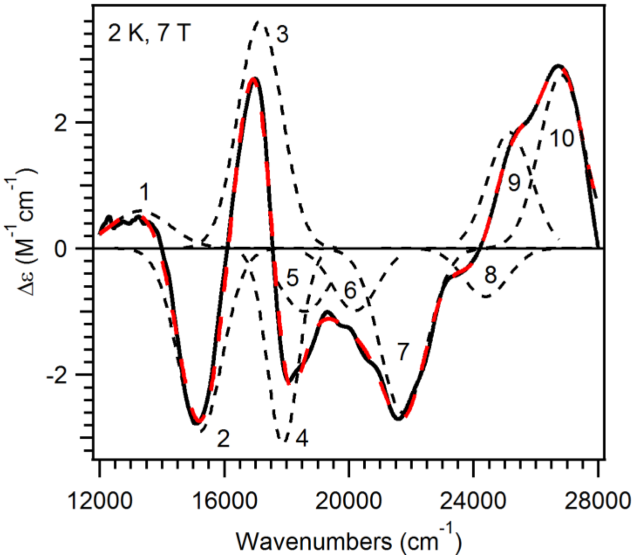

Figure S7. 2 K, 7 T MCD spectrum of a 2.5 mM frozen solution of **3** in PrCN (solid black line) Gaussian bands, and their sum, are shown as dashed black and red lines, respectively.

Table S1. Energy and Widths (fwhm[a]) of Gaussian bands used in the Deconvoluted MCD Spectrum of **3**.

band	energy (cm^{-1})	fwhm (cm^{-1})
1	13 300	2250
2	15 260	1675
3	17 160	1675
4	17 890	1165
5	18 580	1675
6	20 210	1650
7	21 710	1770
8	24 400	1650
9	25 170	1650
10	26 830	1700

[a] fwhm = full width at half maximum.

Table S2. EXAFS fitting results for **3**.

	Mn−O			**Mn−N**			**Mn···C**			**Mn···Mn**			**GOF**
Fit	*n*	*r*	σ^2	*n*	*r*	σ^2	*n*	*r*	σ^2	*n*	*r*	σ^2	*F*
1				6	2.58	3.8							86.7
2	2	1.75	6.2	6	2.58	3.8							76.9
3	2	1.75	6.1	4	2.58	1.8							73.0
4	2	1.78	5.0	4	2.03	15.2				1	2.62	2.5	67.0
5	2	1.78	4.8	3	2.02	10.9				1	2.62	2.5	67.2
6	2	1.80	5.1	2	2.03	3.9				1	2.63	2.3	65.3
				2	2.21	8.9							
7	2	1.80	5.0	2	2.03	3.4				1	2.62	2.2	66.4
				1	2.20	2.5							
8	2	1.80	5.0	3	2.04	7.8				1	2.63	2.4	66.0
				1	2.25	4.0							
9	2	1.79	4.7	2	2.02	4.1	4	2.91	5.7	1	2.63	2.5	58.3
				1	2.19	4.7							
10	2	1.80	4.6	2	2.02	3.0	4	2.85	1.6	1	2.64	1.9	56.1
				1	2.20	2.3	4	2.99	1.8				
11	***2***	***1.79***	***4.2***	***2***	***2.00***	***3.6***	***4***	***2.81***	***4.4***	***1***	***2.63***	***1.8***	***56.6***
				1	***2.17***	***3.7***	***5***	***2.96***	***4.2***				
12	2	1.80	4.3	2	2.02	3.2	5	2.84	4.0	1	2.63	1.7	56.6
				1	2.19	2.9	5	2.98	3.7				
13	2	1.79	4.2	2	2.01	3.3	5	2.82	5.5	1	2.63	1.7	56.9
				1	2.17	3.2	6	2.97	5.1				
14	2	1.79	4.1	2	2.00	4.0	4	2.78	10.6	1	2.62	2.2	57.3
				1	2.16	5.0	8	2.93	8.8				
15	2	1.78	3.9	2	1.98	4.5	4	2.82	3.5	1	2.63	1.9	56.5
				2	2.13	10.2	5	2.97	3.7				
16	2	1.79	4.0	1	1.98	1.8	4	2.82	3.6	1	2.63	1.9	56.2
				2	2.08	9.9	5	2.97	3.7				

Fourier transform range: $k = 2 – 14.3$ Å^{-1} (resolution 0.128 Å). *r* is in Å, σ^2 (Debye-Waller factor) in × 10^3 Å^2, *F* is the weighted goodness-of-fit parameter × 10^2.

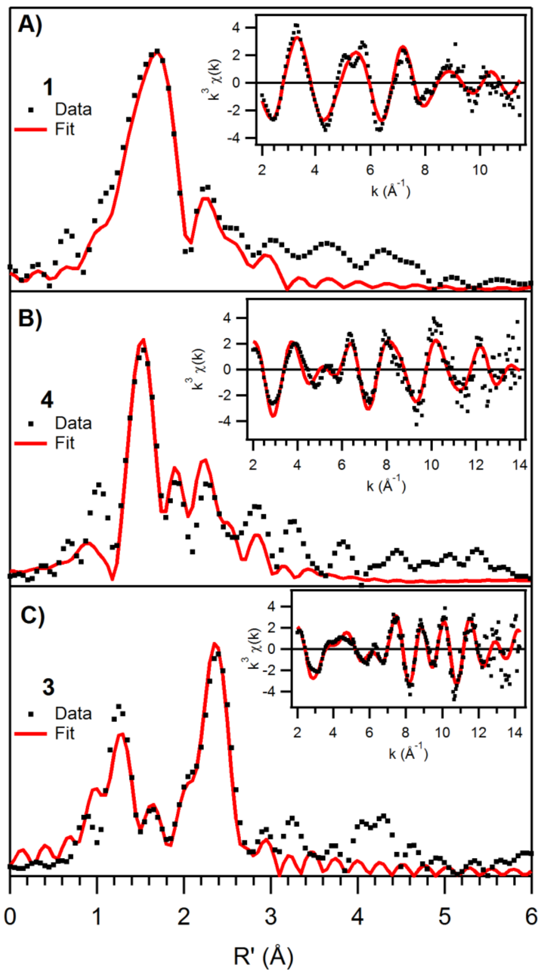

Figure S8. Fourier transforms of Mn K-edge data $k^3\chi(k)$ and EXAFS spectra (inset) for A: $[\mathrm{Mn^{II}(N4py)(OTf)}]^+$ (**1**)[1]; **B**: $[\mathrm{Mn^{IV}(O)(N4py)}]^{2+}$ (**4**)[1]; and **C**: $[\mathrm{Mn^{III}Mn^{IV}(\mu\text{-}O)_2(N4py)_2}]^{3+}$ (**3**), experimental data (dots) and fits (solid). Details regarding fits are given in Table S3.

Table S3. EXAFS fitting results for $[\mathrm{Mn^{III}Mn^{IV}(\mu\text{-}O)_2(N4py)_2}]^{3+}$, $[\mathrm{Mn^{II}(N4py)(OTf)}]^+$, and $[\mathrm{Mn^{IV}(O)(N4py)}]^{2+}$

	Mn – O			**Mn – N**			**Mn • • • C**			**Mn • • • Mn**			**GOF**
	n	*r*	σ^2	*n*	*r*	σ^2	*n*	*r*	σ^2	*n*	*r*	σ^2	*F*
$[\mathrm{Mn^{II}(N4py)(OTf)}]^{+\,a}$	1	2.09	2.4	5	2.26	5.6	3 3	3.00 3.15	7.1 3.8				39.3
$[\mathrm{Mn^{III}Mn^{IV}(\mu\text{-}O)_2(N4py)_2}]^{3+}$	2	1.79	4.2	2 1	2.00 2.17	3.6 3.7	4 5	2.81 2.96	4.4 4.2	1	2.63	1.8	56.6
$[\mathrm{Mn^{IV}(O)(N4py)}]^{2+\,a}$	1	1.69	4.4	4 1	2.00 2.24	6.0 4.4	3 5	2.82 2.97	3.7 3.9				56.1

Fourier transform range for $[\mathrm{Mn^{II}(N4py)(OTf)}]^+$: 2 – 11.5 Å^{-1} (resolution 0.167 Å); $[\mathrm{Mn^{III}Mn^{IV}(\mu\text{-}O)_2(N4py)_2}]^{3+}$: k = 2 – 14.3 Å^{-1} (resolution 0.128 Å); $[\mathrm{Mn^{IV}(O)(N4py)}]^{2+}$: k = 2 – 14.0 Å^{-1} (resolution 0.131 Å). r is in Å, σ^2 (Debye-Waller factor) in 10^3 Å^2, F is a weighted goodness-of-fit parameter x 10^3.

[a] See reference[1].

X-Ray Diffraction Experiments for $[Mn(O)(C_{23}H_{21}N_5)]_2$• 2.8 CF_3SO_3• 0.2 PF_6• 2 CH_3CN (3a).

A full set of unique diffracted intensities (5685 frames with counting times of 5 to 12 seconds and an ω- or ϕ-scan width of 0.50°) was measured[2] for a single-domain specimen using monochromated CuKα radiation (λ= 1.54178 Å) on a Bruker Proteum Single Crystal Diffraction System equipped with Helios multilayer optics, an APEX II CCD detector and a Bruker MicroSTAR microfocus rotating anode x-ray source operating at 45kV and 60mA. Lattice constants were determined with the Bruker SAINT software package using peak centers for 5256 reflections. A total of 13860 integrated reflection intensities having 2θ(CuKα) < 139.58° were produced using the Bruker program SAINT;[3] 5187 of these were unique and gave R_{int} = 0.046. The data were corrected empirically for variable absorption effects using equivalent reflections; the relative transmission factors ranged from 0.629 to 1.000. The Bruker software package SHELXTL was used to solve the structure using "direct methods" techniques. All stages of weighted full-matrix least-squares refinement were conducted using F_o^2 data with the SHELXTL Version 2010.3-0 software package.[4]

All entities appear to be disordered. The Mn(III)/Mn(IV) mixed-valence $\{[Mn(O)(C_{23}H_{21}N_5)]_2\}^{3+}$ cationic dimer utilizes a crystallographic inversion center at (0, ½, ½) in the unit cell. The first triflate anion has two (61%:39%) different orientations in the asymmetric unit. The second triflate is disordered about a crystallographic inversion center at (0, 1, 0) in the unit cell and shares this volume with a $[PF_6]^-$ anion 20% of the time. The final structural model incorporated anisotropic thermal parameters for all nonhydrogen atoms of the metal dimer, CH_3CN solvent molecule, both partial-occupancy orientations for the first $[O_3SCF_3]^-$ anion, the S and three F atoms of the second $[O_3SCF_3]^-$ anion and the P atom of the $[PF_6]^-$ anion. Isotropic thermal parameters were utilized for the oxygen and carbon atoms of the second $[O_3SCF_3]^-$ anion, the F atoms of the $[PF_6]^-$ anion and all hydrogen atoms of the metal dimer and CH_3CN solvent molecule of crystallization.

Surprisingly, even with all of this disorder, a difference Fourier clearly revealed all of the hydrogen atoms bonded to carbon atoms in the dimer. This permitted identification of the non-coordinated nitrogen atom N(5) since it had no significant residual electron density near it but carbon atom C(20) did. The hydrogen atoms were initially included in the structural model as individual isotropic atoms whose parameters were allowed to vary in least-squares refinement cycles. They were later placed at fixed idealized positions (sp^2- or sp^3-hybridized geometry and C-H bond lengths of 0.95 – 1.00 Å) with variable isotropic thermal parameters. The acetonitrile methyl group was incorporated in the structural model as a rigid group (using idealized sp^3-hybridized geometry and C-H bond lengths of 0.98 Å) with idealized "staggered" geometry. The methyl hydrogen atoms were assigned fixed isotropic thermal parameters with values 1.50 times the equivalent isotropic thermal parameter of the methyl carbon atom. The bond lengths and angles for the second triflate and the minor-occupancy (39%) orientation for the first triflate were restrained to have values similar to those for the major-occupancy (61%) orientation of the first triflate anion. Octahedral geometry was imposed on the $[PF_6]^-$ anion by restraining the nonbonded F---F distances to be appropriate multiples of a free-variable P-F bond length that refined to a final value of 1.36(1) Å. The anisotropic thermal parameters of the second triflate sulfur atom, S(2), and the $[PF_6]^-$ phosphorus atom, P, were also restrained to have identical values.

A total of 529 parameters were refined using 68 restraints, 5187 data and weights of $w = 1/ [\sigma^2(F^2) + (0.1982\ P)^2 + (1.2325\ P)]$, where $P = (F_O^2 + 2F_C^2)/ 3$. Final agreement factors at convergence for **3a** are: R_1(unweighted, based on F) = 0.089 for 4319 independent absorption-corrected “observed” reflections having 2θ(CuKα) < 139.58° and I > 2σ(I); R_1(unweighted, based on F) = 0.099 and wR_2(weighted, based on F^2) = 0.262 for all 5187 independent absorption-corrected reflections having 2θ(CuKα)< 139.58°. The largest shift/s.u. was 0.001 in the final refinement cycle. The final difference map had maxima and minima of 0.92 and -0.68 $e^-/Å^3$, respectively.

X-ray Diffraction Experiments for $[Mn(O)(C_{23}H_{21}N_5)]_2$ - 3 PF_6 - 0.5 H_2O (3b).

A full set of unique diffracted intensities (5575 frames with counting times of 5 to 12 seconds and an ω- or ϕ-scan width of 0.50°) was measured[2] for a single-domain specimen using monochromated CuKα radiation (λ= 1.54178 Å) on a Bruker Proteum Single Crystal Diffraction System equipped with Helios multilayer optics, an APEX II CCD detector and a Bruker MicroSTAR microfocus rotating anode x-ray source operating at 45kV and 60mA. Lattice constants were determined with the Bruker SAINT software package using peak centers for 9940 reflections. A total of 47713 integrated reflection intensities having 2θ(CuKα) < 138.44° were produced using the Bruker program SAINT;[3] 9913 of these were unique and gave R_{int} = 0.044. The data were corrected empirically for variable absorption effects using equivalent reflections; the relative transmission factors ranged from 0.745 to 1.000. The Bruker software package SHELXTL was used to solve the structure using “direct methods” techniques. All stages of weighted full-matrix least-squares refinement were conducted using F_o^2 data with the SHELXTL Version 2010.3-0 software package.[4]

Since the second PF_6^- anion (containing phosphorus atom P2) in this structure is bonded to itself across a crystallographic inversion center it must be disordered. A common occupancy factor for the seven nonhydrogen atoms of this anion refined to 0.51. The occupancy factors were therefore fixed at 0.50 in subsequent refinement cycles. The P1 phosphorus atom of the first PF_6^- anion occupies another crystallographic inversion center. There are therefore a total of three (two half occupancy and two full occupancy) PF_6^- anions per Mn dimer and this is critical to the proper identification of the dinuclear cation with Mn(III) and Mn(IV) metals bridged unsymmetrically by two O^{2-} ligands. The asymmetric unit also contains two partial-occupancy water molecules of crystallization in the vicinity of the half-occupancy PF_6^- anion. These water solvent molecules of crystallization are disordered equally between two closely spaced (1.87 Å) sites in the unit cell and presumably represent a half-occupancy water that occupies the same space as the disordered half-occupancy PF_6^- anion; each water oxygen site is occupied a fourth of the time. Whereas the various metric parameters for the anions could have been restrained to have more uniform values, this was not done because it was felt that this might bias the structural results since one must correctly identify the number and nature of the anions in this structure to properly identify the cationic dimer. Nitrogen atoms in the non-coordinated pyridine rings were identified based on the values of equivalent isotropic thermal parameters with all ring atoms modelled as carbon; these also corresponded to the ring orientations observed for compound **3a** where ring hydrogens were observed in a difference Fourier.

The final structural model incorporated anisotropic thermal parameters for all nonhydrogen atoms and isotropic thermal parameters for all hydrogen atoms of the metal dimer. Hydrogen atoms were included in the structural model for the dimer at fixed idealized positions (sp^2- or sp^3-hybridized geometry and C-H bond lengths of 0.95 - 1.00 Å) with isotropic thermal parameters fixed at values 1.2 times the equivalent isotropic thermal parameter of the carbon atom to which they are covalently bonded. The pyridine ring containing carbon atoms C(2B) - C(6B) appears to be disordered between two closely-separated sites. The anisotropic thermal parameters for five carbon atoms [C(3B), C(4B), C(5B), C(6B) and C(22B)] were mildly restrained to have more isotropic values. Hydrogen atoms were not located or included for the disordered partial-occupancy water molecules of crystallization.

A total of 745 parameters were refined using 30 restraints, 9913 data and weights of $w = 1/ [\sigma^2(F^2) + (0.1375\ P)^2 + (39.086\ P)]$, where $P = (F_o^2 + 2F_c^2)/ 3$. Final agreement factors at convergence for **3b** are: R_1(unweighted, based on F) = 0.126 for 7847 independent absorption-corrected “observed” reflections having 2θ(CuKα) < 138.44° and I > 2σ(I); R_1(unweighted, based on F) = 0.146 and wR_2(weighted, based on F^2) = 0.330 for all 9913 independent absorption-corrected reflections having 2θ(CuKα) < 138.44°. The largest shift/s.u. was 0.000 in the final refinement cycle. The final difference map had maxima and minima of 1.91 and -1.13 $e^-/Å^3$, respectively.

Table S4. XRD structural parameters for $[Mn^{III}Mn^{IV}(\mu\text{-}O)_2(N4py)_2](OTf)_{2.8}(PF_6)_{0.2}$ (**3a**) and $[Mn^{III}Mn^{IV}(\mu\text{-}O)_2(N4py)_2](PF_6)_3$ (**3b**)

	$[Mn^{III}Mn^{IV}(\mu\text{-}O)_2(N4py)_2]$ $(OTf)_{2.8}(PF_6)_{0.2}$	$[Mn^{III}Mn^{IV}(\mu\text{-}O)_2(N4py)_2](PF_6)_3$
	3a	**3b**
Empirical formula	$C_{52.80}H_{48}F_{9.60}Mn_2N_{12}O_{10.40}P_{0.20}S_{2.80}$	$C_{46}H_{42}F_{18}Mn_2N_{10}O_{2.50}P_3$
Formula weight	1405.27	1319.69
Temperature	100(2) K	100(2) K
Wavelength	1.54178 Å	1.54178 Å
Crystal system	Triclinic	Monoclinic
Space group	$P\bar{1} – C_i^1$ (No. 2)	$P2_1/c – C_{2h}^5$ (No.14)
Unit cell dimensions	a = 11.0548(5) Å	a = 25.7399(6) Å
	b = 11.7210(4) Å	b = 12.5771(3) Å
	c = 12.1500(4) Å.	c = 17.9093(4) Å
	α = 96.673(2)°	α = 90°
	β = 105.695(3)°	β = 105.4270(10)°
	γ = 91.203(3)°	γ = 90°
Volume	1503.1(1) $Å^3$	5588.9(2) $Å^3$
Z	1	4
Density (calculated)	1.552 Mg/m^3	1.568 Mg/m^3
Absorption coefficient	5.235 mm^{-1}	5.472 mm^{-1}
F(000)	716	2660
Crystal size	0.13 x 0.06 x 0.01 mm^3	0.08 x 0.07 x 0.02 mm^3
Theta range for data collection	3.80 to 69.79°.	3.56 to 69.22°.
Index ranges	-13<=h<=11	-30<=h<=30
	-14<=k<=10	-12<=k<=14
	-14<=l<=14	-20<=l<=21
Reflections collected	13860	47713
Independent reflections	5187 [R(int) = 0.046]	9913 [R(int) = 0.044]
Completeness to theta = 66.00°	94.6 %	97.9 %
Absorption correction	Multi-scan	Multi-scan
Max. and min. transmission	1.000 and 0.629	1.000 and 0.745
Refinement method	Full-matrix least-squares on F^2	Full-matrix least-squares on F^2
Data / restraints / parameters	5187 / 68 / 529	9913 / 30 / 745
Goodness-of-fit on F^2	1.015	1.092
Final R indices [I>2sigma(I)]	R_1 = 0.089, wR_2 = 0.250	R_1 = 0.126, wR_2 = 0.319
R indices (all data)	R_1 = 0.099, wR_2 = 0.262	R_1 = 0.146, wR_2 = 0.330
Largest diff. peak and hole	0.92 and -0.68 e/$Å^3$	1.91 and -1.13 e/$Å^3$

$R_1 = \Sigma \|F_o| - |F_c\| / \Sigma |F_o|$

$wR_2 = \{ \Sigma [w(F_o^2 - F_c^2)^2] / \Sigma [w(F_o^2)^2] \}^{1/2}$

References

1. D. F. Leto, R. Ingram, V. W. Day and T. A. Jackson, *Chem. Commun.*, 2013, **49**, 5378-5380.

2. *Data Collection: SMART Software Reference Manual.*, Bruker-AXS. 5465 E. Cheryl Parkway, Madison, WI 53711-5373 USA, 1998.

3. *Data Reduction: SMART Software Reference Manual.*, Bruker-AXS. 5465 E. Cheryl Parkway, Madison, WI 53711-5373 USA, 1998.

4. *Refinement: SHELXTL v2010.3-0. Bruker-AXS*, 5465 E. Cheryl Parkway, Madison, WI 53711-5373 USA.